The art of UHF RFID antenna design: impedance matching and size-reduction techniques

Published in IEEE Antennas and Propagation Magazine, Vo.50, N.1, Jan. 2008

Gaetano Marrocco
Dipartimento di Informatica Sistemi e Produzione
University of Roma "Tor Vergata"
Via del Politecnico, 1, 00133, Roma
Tel:+39 06 72597418, Fax:+39 06 72597460
Email: marrocco@disp.uniroma2.it

Abstract

Radio Frequency Identification technology based on the reader/tag paradigm is quickly permeating several aspects of the everyday life. The electromagnetic research mainly concerns the design of tag antennas having high efficiency and small size and suited to complex impedance matching to the embedded electronics. Starting from the available but fragmented open literature, this paper presents a homogeneous survey of relevant methodologies for the design of UHF passive tag antennas with particular care to illustrate, within a common framework, the basic concepts of the mostly used design layouts. The design techniques are illustrated by means of many non-commercial examples.

Keywords*:* antenna design, RFID, tag, T-match, meander line antenna, impedance matching, miniaturized antenna, PIFA, IFA.

1. Introduction

The idea of Radio Frequency IDentification (RFID) of objects and remote control of devices was first introduced in the late 1948 by H. Stockman [1]. After the big efforts given by the development of the microelectronic technology in the 1970s [2], and the continuing evolutions of the last decade [3], [4], RFID is now imposing as a pervasive technology [5], [6] in everyday life [7] and in more advanced applications involving logistics, inventory management, aided systems for disabled people, homeland and personal security, distributed sensor networks [8] and mobile healthcare [9]. A basic RFID system comprises a radio-scanner unit, called *reader*, and a set of remote transponders, denoted as *tags*, which include an antenna and a microchip transmitter with internal read/write memory. In passive tags, the required energy to drive the microchip comes from the interrogation system itself and a backscattering modulation is achieved when the microchip acts as a switch to match or mismatch its internal load to the antenna.

Several frequency bands have been standardized for this technology. Low frequency (LF, 125-134 kHz) and high frequency (HF, 13.56 MHz) systems are the most mature and worldwide diffused technology. They are based on quasi-static magnetic flux coupling among the reader's and tag's coils. Ultra-high frequency (UHF, 860-860 MHz) and microwave (2.4 GHz and 5.8 GHz) systems involve instead electromagnetic interaction among true antennas, permit longer communication links and they are the emerging technology.

Together with the microchip power sensitivity, the tag antenna plays a key role in the overall RFID system performances, such as the overall size, the reading range and the compatibility with the tagged objects. Most of the antennas for UHF omnidirectional tags are commonly fabricated as modified printed dipoles. The design goal is to achieve inductive input reactance required for the microchip conjugate impedance matching, and to miniaturize the antenna shape. Several tricks are used, and the resulting tags sometimes exhibit charming and nearly artistic layouts.

Although many tag configurations can be retrieved in the scientific papers, or even in the catalogs of commercial products, there is a lack of systematization of the design methodology. A first tutorial paper is available in [10], where the concept of conjugate impedance matching to the microchip is reviewed, some performance parameters are introduced and fabrication and measurement procedures are described in some detail.

This paper provides a unitary and general survey of the most used design procedures for miniaturized tag antennas with complex impedance matched to the microchip load. Attention is devoted to the rationale and to the main features of basic configurations, by whose modification and combination a great variety of tag layouts can be easily obtained. For each design solution, the role of the main geometrical parameters over the complex impedance tuning it is here investigated by introducing *matching charts* which are a useful tool to suite a same antenna configuration to different kinds of microchip.

The rest of the paper is organized into four main Sections. Section 2 introduces several techniques to achieve complex impedance matching, such as the T-mach, the proximity-loop and nested-slot layouts. Then (Section 3), miniaturization and bandwidth issues are addressed with references to meandered and inverted-F solutions corroborated by many examples. Other miscellaneous design issues are addressed in Section 4 and, finally, some measurement and test procedures for UHF tag are presented in Section 5.

2. Methods for conjugate impedance matching

Having fixed the effective power ($EIRP_R$) transmitted by the reader and the sensibility (P_{chip}) of the tag's transponder, e.g. the RF power required to the microchip electronics to turn on and to perform back-scattering modulation, the maximum activation distance of the tag along the (θ,ϕ) direction [10], under the hypothesis of polarization matching between reader and tag antennas, is given by

$$d_{\max}(\theta,\phi) = \frac{c}{4\pi f}\sqrt{\frac{EIRP_R}{P_{chip}}\tau G_{tag}(\theta,\phi)} \tag{1}$$

where $G_{tag}(\theta,\phi)$ is the tag gain and the factor

$$\tau = \frac{4R_{chip}R_A}{|Z_{chip}+Z_A|^2} \le 1 \tag{2}$$

is the *power transmission coefficient* which accounts for the impedance mismatch between antenna ($Z_A=R_A+jZ_A$) and microchip ($Z_{chip}=R_{chip}+jZ_{chip}$). The microchip impedance depends on the input power and, since the transponder includes an energy storage stage, its input reactance is strongly capacitive and most of the available RFID ASICS in the UHF band exhibit an input reactance roughly ranging from -100Ω to -400Ω [11], [12], [13], while the real part is about an order of magnitude smaller or less. The antenna impedance should be inductive in order to achieve conjugate matching, and a large impedance phase angle, $atan(Z_A)>45°$, needs to be obtained. Beyond d_{max} the power collected by the tag decreases below the microchip sensibility and the tag becomes unreachable.

To obtain low-cost devices, it is not feasible to use external matching networks involving lumped components and therefore the matching mechanisms have to be embedded within the tag antenna layout.

Several feeding strategies can be adopted for antenna tuning. The most used are modified versions of the well-known T-match, the proximity coupling to a small loop, and the inclusion of shaped slots. Useful configurations should permit a nearly independent tuning of resistance and reactance when acting on the tag geometrical parameters.

Some matching techniques will be now reviewed and compared having fixed, for clarity, the antenna maximum size to half a wavelength without taking care to the overall size which could be eventually un-practicable for real applications. The miniaturization issues are deferred to the next Section.

The matching capability of the considered feeding schemes will be summarized through an impedance charts where the input resistance and reactance are related to the variation of relevant geometrical parameters. A matching scheme is as more agile as the iso-lines for resistance and reactance are mutually parallel. The basic matching schemes are illustrated with the help of some non-commercial examples taken from the recent open scientific literature.

2.1 T-match

With reference to Figure 1, the input impedance of a (planar) dipole of length *l* can be changed by introducing a centered short-circuit stub, as detailed explained in the old book [14], and more recently resumed in [15]. The antenna source is connected to a second dipole of length $a \le l$, placed at a close distance *b* from the first and larger one. The electric current distributes along the two main radiators according to the size of their transverse sections.

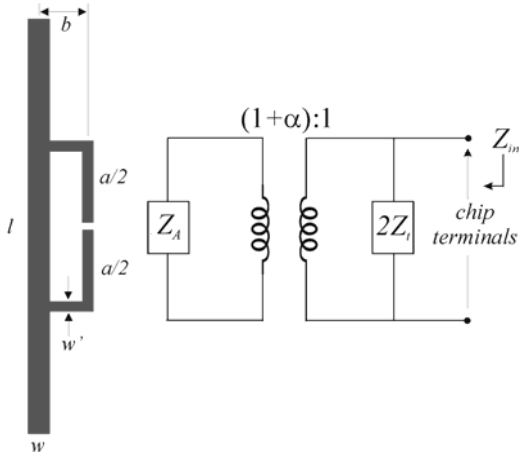

Figure 1: T-match configuration for planar dipoles and equivalent circuit where the impedance step-up ratio (1+α) is related to the conductors' cross-sections.

It can be proved, [14], [15] that the impedance at the source point is given by

$$Z_{in} = \frac{2Z_t(1+\alpha)^2 Z_a}{2Z_t + (1+\alpha)^2 Z_a} \tag{3}$$

where $Z_t = jZ_0 \tan ka/2$ is the input impedance of the short-circuit stub formed by the T-match conductors and part of the dipole; $Z_0 \cong 276\log_{10}(b/\sqrt{r_e r_e'})$ is the characteristic impedance of the *b*-spaced two-conductors transmission line; Z_A is the dipole impedance taken in its centre in the absence of the T-match connection; $r_e=0.25w$ and $r_e' = 8.25w'$ are the equivalent radii of the dipole and of the matching stub, supposed to be planar traces, and $\alpha = \ln(b/r_e')/\ln(b/r_e)$ is the current division factor between the two conductors.

The geometrical parameters *a*, *b* and the trace's width *w'* can be adjusted to match the complex chip impedance Z_{chip}. The T-match acts as an impedance transformer (Figure 1). In case of half a wavelength

dipoles, the resulting input impedance at the T-match port is inductive, while for smaller dipoles, the total input impedance can be both capacitive and inductive.

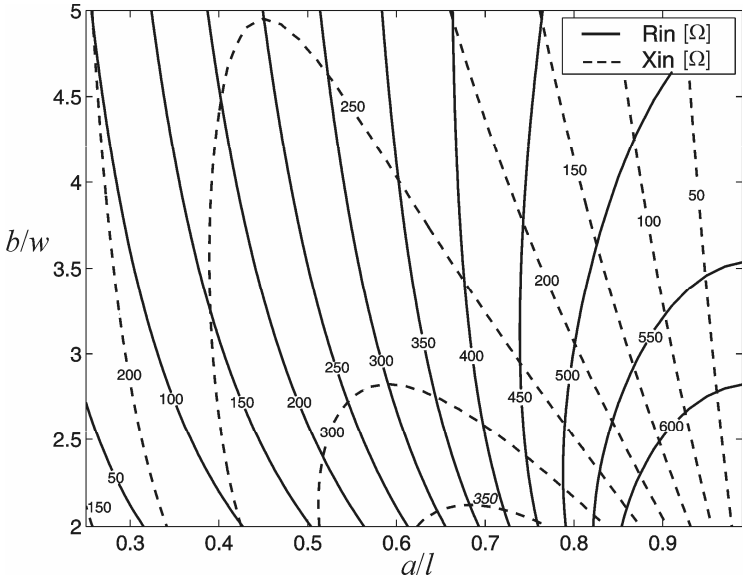

Figure 2: Matching chart for the T-match in Figure 1, in the case l=λ/2, w= λ/100, w'= w/3 and Z_A=75Ω.

For example, Figure 2 shows a matching chart for the T-match layout having fixed the ratio between the dipoles cross-sections to w/w'=3. The input resistance and inductance depend on both the stub size a and b, but with different rules. It is known that the cross-section of the second conductor plays a considerable effect on the resulting antenna impedance. In particular, it can be easily verified from (3) that the increase of the w/w' ratio will raise the impedance values, and the iso-lines for resistance and reactance become nearly vertical and mutually parallel (strong dependence on b size) resulting in a reduced matching agility. Even with small values of a and b, high values of input resistance are generally found, making difficult the impedance matching to real microchip transmitters unless some shape modification of the main radiator are considered. A single T-match layout could be therefore not completely adequate to match high impedance-phase-angle microchips. In such cases, further degrees of freedom are added by means of multiple T-match stages. The T-match geometry can be also embedded within the main radiator yielding a compact structure as in Figure 3.

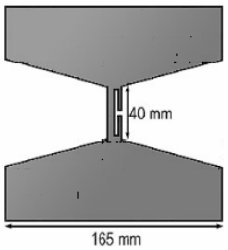

Figure 3: Example of embedded T-match feed. This antenna has been proposed in [16] to be rolled around cardboard reels.

2.2 Inductively coupled loop

Instead of the T-match, the radiating dipole may be sourced via an inductively coupled small loop [17] placed at a close proximity to the radiating body (Figure 4). The terminals of the loop are directly connected to the microchip. This arrangement adds an equivalent inductance in the antenna. The strength of the coupling, and therefore of the added reactance, is controlled by the distance between the loop and the radiating body as well as by the shape factor of the loop.

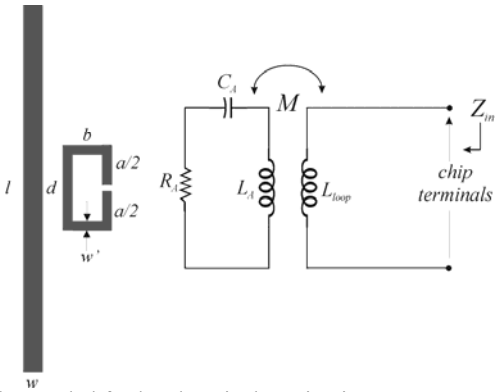

Figure 4: Layout of the inductively coupled feed and equivalent circuit. Parameters R_A, C_A, L_A gives the circuit model of the radiating body near its (series) resonance.

The inductive coupling can be modeled by a transformer and the resulting input impedance seen from the loop's terminals is

$$Z_{in} = Z_{loop} + \frac{(2\pi f M)^2}{Z_A} \tag{4}$$

where $Z_{loop} = j2\pi f L_{loop}$ is the loop input impedance. Whether the dipole is at resonance, the total input reactance depends only on the loop inductance L_{loop}, while the resistance is related to the sole transformer mutual inductance M:

$$\begin{aligned} R_{in}(f_0) &= (2\pi f_0 M)^2 / R_A(f_0) \\ X_{in}(f_0) &= 2\pi f_0 L_{loop} \end{aligned} \tag{5}$$

Under the assumption that the radiating body is infinitely long, the loop inductance and mutual coupling M can be expressed in terms of the loop size and of its distance from the dipole through analytical formulas [18]. It is important to note that the mutual coupling, and therefore the total input resistance is dependent on both the loop shape and on the dipole-loop distance, while the reactance L_{loop} is mainly affected by the only loop's aspect ratio.

Figure 5 shows an example of matching chart, computed by Method of Moments [19], for the loop-driven dipole, in the particular case of resonant dipole and square loop (a=b). As expected from (3), the input reactance is nearly un-affected by the loop-dipole distance (d) and the corresponding iso-lines are vertical. For a fixed size of the loop, the resistance reduces when the loop-dipole distance increases. A design procedure could therefore initially select the loop size with the purpose to cancel the chip capacitive reactance, and further on a proper loop-dipole distance d is chosen to match the chip resistance. This layout is particularly effective for microchips having high impedance phase angle.

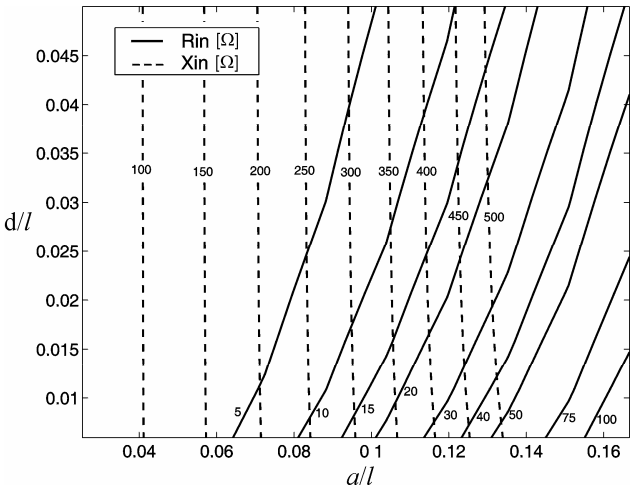

Figure 5: Matching chart for the loop-fed dipole in Figure 4 having fixed $l=\lambda/2$, $w=\lambda/100$, $w'=w/3$ and $a=b$ (square loop).

2.3 Nested slot

A completely different matching strategy, useful for tag fabricated with large planar dipoles or suspended patches, [20], [21] may employ a nested shaped slot (Figure 6-left). Thanks to the inductive reactance of a non-resonant slot, this feeding strategy has relevant capability of complex impedance matching even when the tag is attached onto high-permittivity substrates (see for instance Figure 6-right). The slot profile can be seen as a slot-line impedance transformer, where each discontinuity (tooth) provides energy storage and radiation. By increasing the number of teeth, further degrees of freedom are added with the possibility to improve miniaturization and a achieve multi-band features [22].

Since the slot sizes may be comparable with the patch surface, the radiation features are related to both the objects. In particular, the maximum antenna gain is mainly fixed by the patch side *l*, while the impedance tuning can be changed by acting on the slot's aspect ratio *a* and *b*.

Depending on the shape and on the size of the internal slot, the antenna mainly acts either as a *H*-slot, a broadband dipole or as a doubly folded dipole.

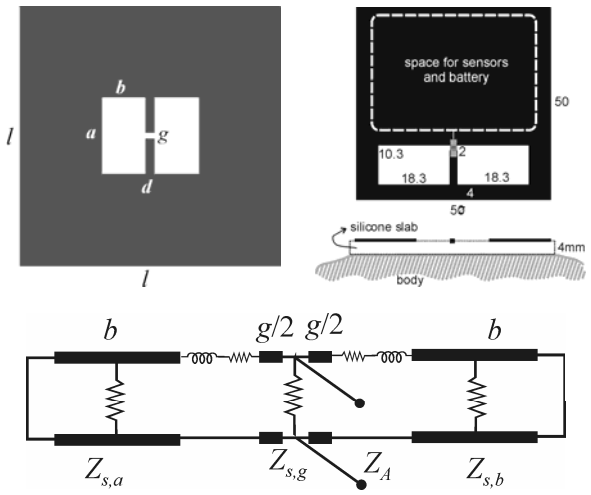

Figure 6: up) Geometry of the nested-slot suspended-patch and example of tag (size in [mm]) to be attached onto the human body and able to host sensors [20]. Down) equivalent simplified distributed circuit.

When the slot width *b* is really smaller than the external side *l*, a typical RLC behavior can be observed with strong reactance peaks. As the size *b* increases, the resonance moves toward the DC and the reactance peak reduces.

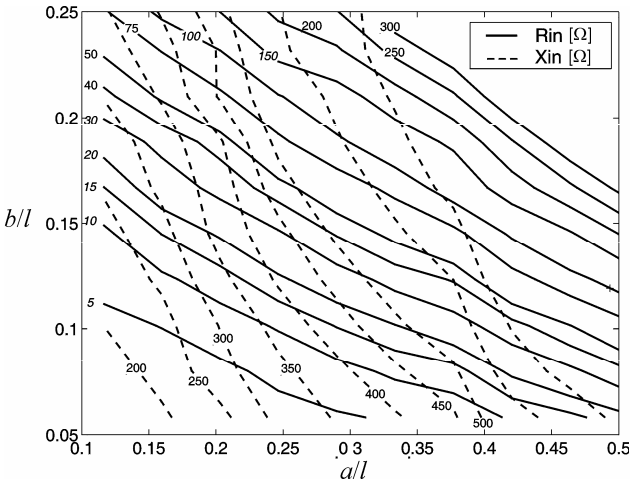

Figure 7: Matching chart for the nested slot matching layout in Figure 6 in the case of $l=\lambda/2$ and $d=g=\lambda/150$.

It has been observed [20] that, in case the slot width is nearly similar to the antenna side ($2b \approx l$), the input reactance is slowly variable with the frequency, and therefore the tag can remain well tuned within a wide band. When the sizes *a* and *b* increase ($2b \approx a \approx l$) until the slot fills nearly the whole patch surface, a folded dipole mode is achieved. Figure 7 shows the matching chart of the nested-slot suspended-patch when the H-slot aspect ratio $\{a, b\}$ is changed. It can be observed that the resistance is manly sensitive to the slot width *b* while the reactance presents fast and nearly linear variations along with both *a* and *b* sizes. The impedance

iso-lines yield a nearly orthogonal grid and therefore a broad resistance dynamics can be obtained for any fixed reactance value, with a high degree of matching capability.

3. Methods for size reduction

Since most of the UHF RFID tags have to be attached over small objects, the antenna geometry needs to be miniaturized without un-acceptable degradation of the radiation efficiency. Two size-reduction strategies, successfully used to design RFID tags, are now reviewed: meandering and inverted-F structures. Both require a single of even multiple folding of the radiating body, but the inverted-F antennas additionally include a finite approximation of a ground plane.

Whereas the design of simple tag layouts can be accomplished by using the previously introduced matching charts, geometries with a large number of parameters, as those described next, often require non-deterministic optimization tools such as those based on the Genetic Algorithms [23].

3.1 Meandering

As proposed in [24], by folding the arms of a dipole antenna along a meandered path (Figure 8), a wire configuration is produced with distributed capacitive and inductive reactances which globally affect the antenna input impedance. Up to the first antenna resonance, the currents on the adjacent horizontal segments of the Meander Line Antennas (MLA) have opposite phases. These transmission line currents do not give valuable contribution to the radiated power, but nevertheless produce losses. Resonances are achieved at much lower frequencies than in the case of a straight dipole of the same height at the expense of a narrow bandwidth and a low efficiency.

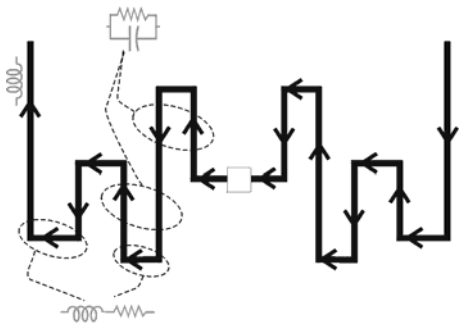

Figure 8: Geometry of a Meander Line Antenna having multiple unequal turns. Horizontal lines mainly control the radiation resistance; adjacent vertical lines (transmission-line current mode) give storage of electric energy and loss; the overall conductor length affects the inductance.

Figure 9 shows some relevant examples of RFID tag antennas found on recent scientific publications, which use the meander-line technique to reduce the size.

(a) Equi-spaced MLA (*f*=953MHz) with T-match feed, [25].
(b) MLA (*f*=915MHz) with inductively coupled loop feed, [26].
© Equi-spaced MLA (*f*=920MHz) with a loading bar. Antenna reactance and resistance can be controlled by trimming the MLA and the bar by means of punching holes [10], [27].
(d) The *Albano* tag (*f*=915MHz) which is a doubly-folded *L*-shaped dipole useful to be wrapped around the corner of a box with the purpose to achieve nearly omnidirectional visibility, [28].

(e) Multi-conductor antenna (*f*=900MHz) with a double T-match scheme and spiral folding used to achieve the required inductance. The additional external conductor permits to increase the antenna bandwidth especially when it is attached on a dielectric slab or on a metal object [29].
(f) Text-shaped MLA (*f*=870MHz) tag where the turns are obtained by joining the adjacent letters of a text, [30].
(g) Resonant tapered dipole (*f*=915MHz), partially meandered, provided with a resistive shorting stub and a double inductive stub to achieve impedance matching. The conductor tapering is aimed to obtain a smoother transition from the connecting pads of the microchip to the dipole arms and to maintain the high-efficiency when the antenna is embedded in a dielectric, [12].
(h) Multi-conductors meander line tag (*f*=900MHz) with circular-shaped double T-match. The particular MLA layout is such to put in phase most of the horizontal currents [31].

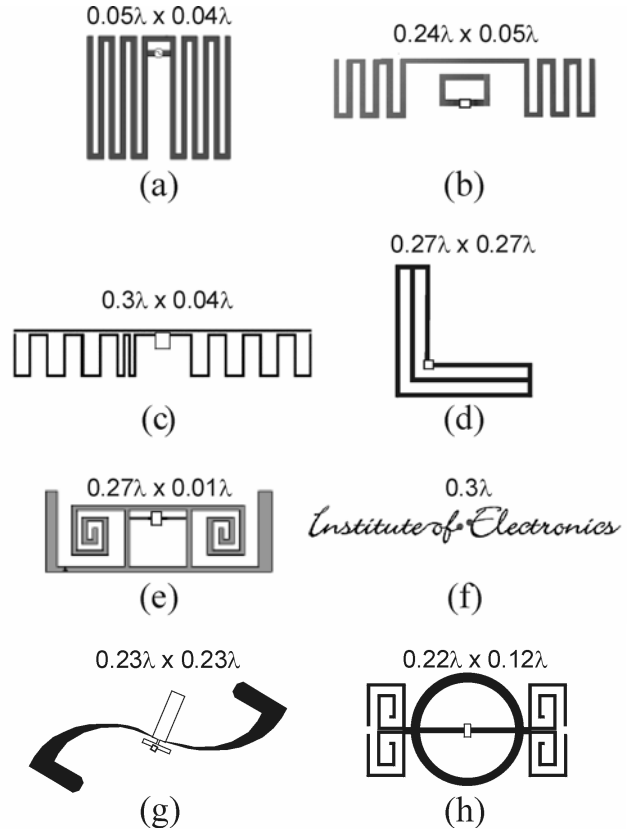

Figure 9: Examples of tag antennas including multiple meanders and both T-match and loop-coupling feeds. Sizes are reported in wavelengths.

The shape of the meanders can be periodic, as in most of the above examples, or even individually optimized to match a particular impedance. At this purpose, the required inductive reactance may be achieved by allocating within a small space a wire (or strip) conductor longer than half a wavelength. Reduction of the antenna height down to fractions of a wavelength can be easily achieved, as shown for example in Figure 10. In this case the meanders' shape has been chosen by the Genetic Algorithm procedure in [24] with the purpose to maximize the realized gain τG_{tag}, having constrained the tag size within a λ/5xλ/5 square. Since the linear conductor's length of the optimized MLAs is generally longer that half a wavelength, the tag maximum gain may be nearly the same of a regular resonant dipole in spite of the consistent size reduction. As expected, the total length of the MLA increases along with the reactance to be matched, while the antenna height controls the resistance.

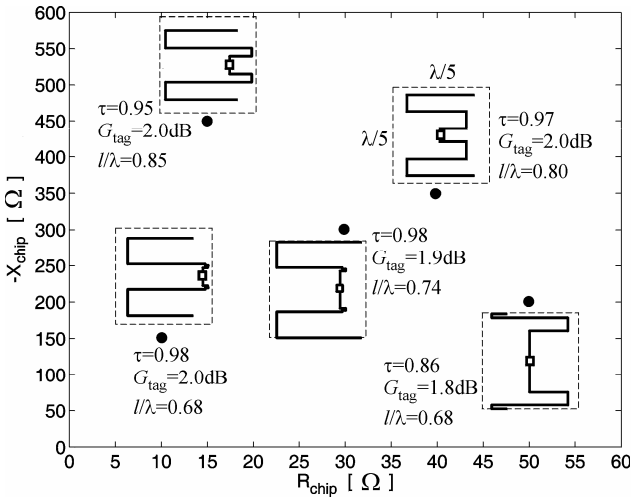

Figure 10: Meander line antennas with maximum size λ/5xλ/5 matched to some complex impedances (black circles). *L* indicates the total length of the MLA conductor supposed to be in copper. Trace width: λ/300.

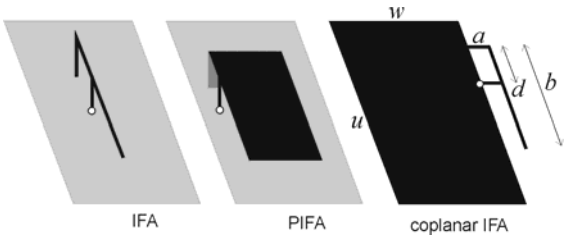

Figure 11: Folded antennas. The circles indicates the position of the microchip. In the rightmost, the inverted-F is placed on the same layer of the ground plane (coplanar layout).

3.2 Inverted-F configurations

The size of a vertical wire monopole can be reduced by folding, parallel to the ground plane, part of the wire according to an inverted-L structure which has typically low resistance and a high capacitive reactance. To provide tuning freedom, the structure is augmented with a shorting pin, giving the F-type (IFA) configuration (Figure 11). This can be also viewed as a monopole version of the T-match, whether the radiating body is folded to reduce the space occupation. In the inverted structure the radiating elements are mainly the conductors orthogonal to the ground plane, while the folded conductor, together with its image, yields a transmission line current mode producing power loss and only negligible radiation. This kind of geometry therefore does not exhibit high efficiency. The antenna bandwidth can be improved by replacing the wires with large strips (Planar Inverted-F Antenna – PIFA). Due to the presence of a ground plane, these configurations are suited to host additional electronics and sensors or to be attached over a high-conductivity object. The introduction of additional conductors, orthogonal to the ground, may permit to obtain multi-band tags. Coplanar geometries, e.g. such that the inverted-F and the ground plane lay on a same layer, are also used [32] with the purpose to simplify the fabrication and the microchip connection. In such a case, the resulting geometry con be seen as an asymmetric dipole where the arms are given by the inverted-F and the ground plane whose size is about a quarter of wavelength.

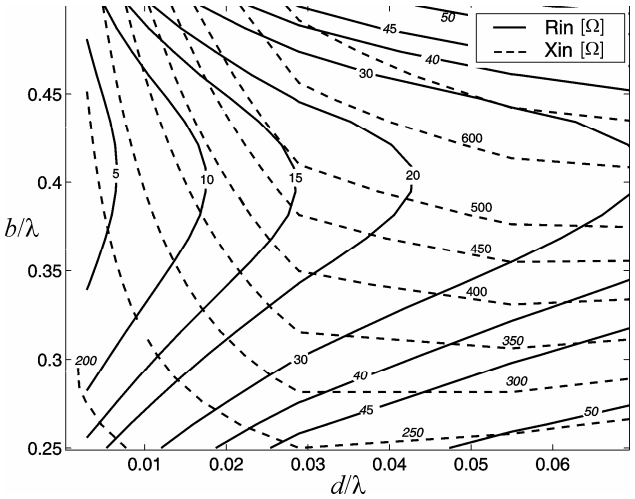

Figure 12: Matching chart for the coplanar IFA geometry of Figure 11 having fixed w=λ/4, u= λ/2, a= λ/10 and changing the folded wire length and the feeding position. Width of the IFA linear conductors: λ/600.

A wide spectrum of complex input impedances can be obtained by varying the geometrical parameter {a, b, d}. As shown in the matching chart of Figure 12, the input (inductive) reactance monotonically increases with both b and d. The resistance, instead, enlarges along with d while it undergoes changes with respect to b around a local minimum value. It could be therefore possible to find two different useful layouts, for a given input impedances, having relevant differences in the size b (length of the conductor parallel to the ground). Finally, the antenna becomes more inductive as the radiating conductor a increases since the folded part of the antenna moves away from the ground plane. The matching dynamics seems to be comparable to that of the nested-slot suspended-patch configuration.

Some examples of inverted-conductor tags, coming from recent scientific papers, are shown in Figure 13 and summarized in the following.

(a) A conventional two-layers PIFA (f=870MHz) with square conductor. The tag microchip is attached vertically onto the dielectric truncation, [33].
(b) Two-layers double PIFA tag with proximity loop feed (f=900MHz). The microchip is placed on the top metallization. The loop is fully integrated within the top conductors, [34].
(c) Coplanar IFA (f=870MHz) with additional horizontal stub, [35].
(d) Coplanar IFA (f=2450MHz) with multiple folded conductors to obtain dual band operations at 2400 MHz and 5300 MHz, [36].

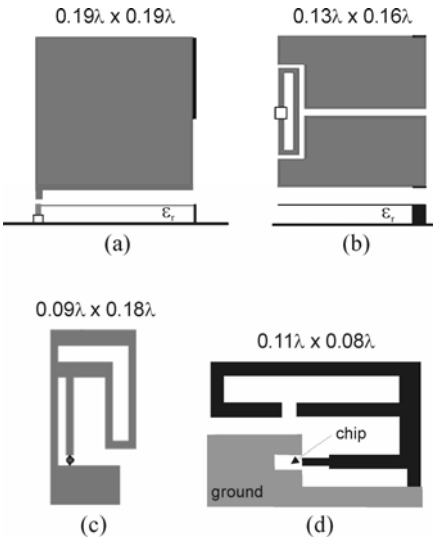

Figure 13: Examples of modified PIFA and IFA tags with single and multiple foldings. The tag sizes are indicated in wavelength fractions.

3.3 Bandwidth issues

Unlike conventional 50 Ω-matched antennas, the most useful parameter for the definition of RFID tags' bandwidth is the realized gain, rather than the return loss, as also in the design of ultra-wideband antennas [37]. In fact, the tag bandwidth depends on the required minimum read range in the specific application and, once fixed the power constraints, it can be therefore related to the system parameter τG_{tag}. The stability of the realized gain over the frequency gives indeed the *rangewidth* of the reader-tag system.

In general, it is well known that antenna miniaturization yields layouts with reduced bandwidth. Although RFID applications involve narrow frequency bands, bandwidth issues are nevertheless important since tag impedance may be easily detuned by the coupling with the objects to be tagged, as well as by the interaction with the surrounding environment, and the resulting reading range could be globally degraded.

At the purpose to introduce a general bandwidth definition, not dependent on the particular application, a perfectly matched isotropic antenna ($[\tau G_{tag}]_0=1$) is selected as reference. The tag band is then defined as the frequency range, $[f_{min}, f_{max}]$, where the following condition holds:

$$[\tau G_{tag}](f) = \frac{1}{2}[\tau G_{tag}]_0(f_c) \tag{6}$$

f_c being the middle-band frequency. Under his condition, the activation range reduces to not more than the 70% of the activation range of the reference antenna. This definition permits to compare the features of different tags whatever the transmitter power and the microchip sensitivity are. Whether the tag is designed to be attached over a high-loss target, as in the case of human body, a different reference antenna (lower) gain my be chosen.

To discuss the bandwidth capability of miniaturized tags, an MLA and an IFA antenna, having maximum size not exceeding 5 × 5cm (about λ/7 at 870 MHz), and matched to a high impedance phase angle microchip (Z_{chip}=15-j450Ω), are now analyzed with respect to frequency changes. With reference to Figure 14 the IFA vertical conductors occupy most of the available space with the purpose to achieve the required input resistance. The MLA antenna has been automatically optimized as previously discussed. In particular, under the only constraint of best realized gain, the solution found by the genetic optimizer is slightly smaller than the imposed maximum size. No bandwidth constraint have been considered.

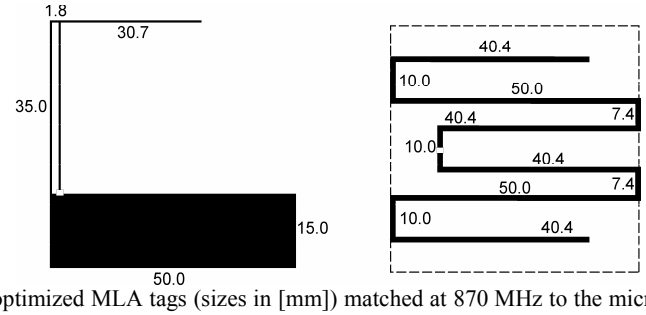

Figure 14: IFA and GA-optimized MLA tags (sizes in [mm]) matched at 870 MHz to the microchip impedance Z_{chip}=15-j450Ω. The maximum external size are 5×5cm (≈0.14λ). Trace size: 1mm.

Figure 15 shows the tags' features (maximum gain, power transmission factor and realized gain) with respect to the frequency variation. The MLA exhibits a gain larger than the IFA's one. The gain is nevertheless only slightly frequency dependent and therefore the bandwidth performances are manly affected to the impedance matching. The MLA geometry permits a better realized gain (τG_{tag} =1.46) at 870 MHz than the IFA design (τG_{tag} =1.33) but the activation range improvement at that frequency if only of 5%.

According to the above definition, the band features of the considered examples are reported in Tabella 1, where $\Delta f = f_{max} - f_{min}$ and $B = \Delta f / f_c$. Although the two antennas show a nearly similar narrow band, as expected by the relevant size reduction, the IFA layout has a slightly broader relative bandwidth. It is however to consider that the MLA layout possesses a larger number of degrees of freedom, if compared to the standard IFA, and therefore additional constraints may be included in the MLA optimization procedure at the purpose of bandwidth enhancement.

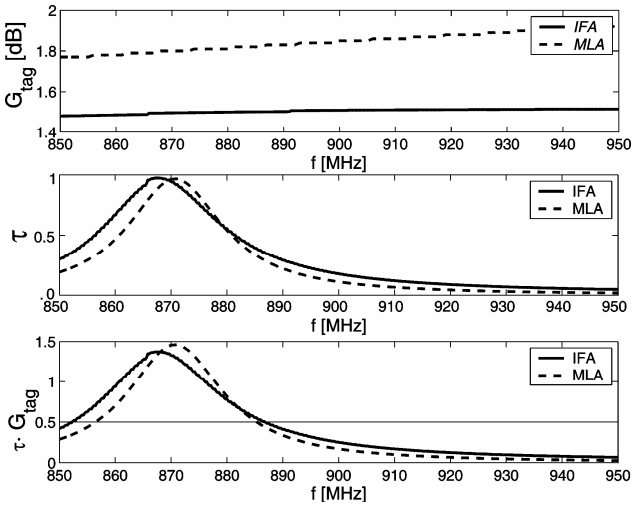

Figure 15: Maximum gain and power transmission coefficients, vs. frequency, for the IFA and MLA tags having the same overall size (5×5cm). The horizontal thin line for τG_{tag} =0.5 permits to appreciate the tag bandwidth within which the activation distance is not less than the 70% the activation distance of a reference perfectly matched isotropic antenna.

Tabella 1: Bandwidth features of the 870MHz MLA and IFA tags having the same maximum external size 5×5cm.

		MLA	**IFA**
f_{min}	[MHz]	856	852
f_{max}	[MHz]	885	887
Δf	[MHz]	29	35
B	**[%]**	3.3	4.0

4. Others designs (dual-band, dual polarization and near-field tags)

Some issues concerning the design of particular tags which are not fully comprised in the previous classification, such as dual-band and dual-polarized tags and the new near-field UHF tags, are now shortly discussed.

3.1 Dual-band Tags

Multi-band operation is traditionally achieved in antennas by using several resonant elements or exploiting high order harmonics. Some dual-band design solution have been recently proposed to achieve 870MHz and 2.45GHz or 2.45 GHz and 5.8 GHz compact multifunction transponders. The basic idea is to load a traditional tag antenna with parasitic tuning elements such as inner slots or tuning stub. The goal is to avoid a size increase, and the tuning elements are engineered to be embedded inside the radiating element itself. Figure 16 shows four examples of dual band tags.

a) A planar antenna [38] with shaped slots used to both achieve two working frequencies (resonances or complex impedance matching) at 868MHz and 2450 MHz, and to reduce the antenna size at the smaller frequency
b) Microstrip Sierpisky Gasket printed antenna [39] optimized for dual band operations at 2.45 GHz and 5.8 GHz. A microstrip line feeds the first iteration of the Sierpinsky fractal metallization and the ground plane under the radiating element is removed. The metallic triangle's size fixes the fundamental mode while the inner triangular slot the second resonance.
c) Slot-loaded dipole [40], for operations at 870MHz and 2450 MHz . A coupled slot is here introduced within the dipole conductor whose global length fixes the lower working frequency. The slot acts as a sort of current trap [41] which breaks off the dipole into a smaller length conductor working at the higher frequency. Additional slots, or any other lumped and distributed impedance, can be introduced to further tune the impedance.
d) PIFA with open tuning stub [42]. By changing the width and the length of the stub, the antenna impedance can be matched to the microchip at two different frequencies (870 MHz, 915 MHZ) at same time.

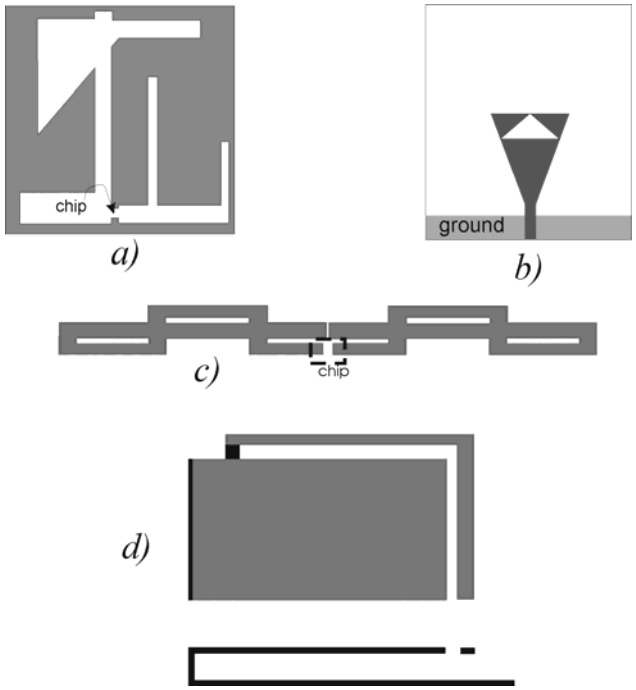

Figure 16: Examples of dual-band tag designs.

3.2 Dual-polarization Tags

Dual polarized tag antennas are generally designed either to reduce the read distance sensibility to the mutual orientation between the reader and the tag, or to receive energy and transmit back the identification information through different antennas and polarizations. In these designs orthogonal slots [43], driving a conventional patch tag, or also crossed dipoles [44], can be used.

4.3 Near field UHF Tags

Very recently, some attention has been devoted to UHF tags able to work in the reader's near field as a possible solution to item level tagging in pharmaceutical and retailing industry (see the overview, and the related references, in [45]). When compared to the well assessed LF RFID systems, the near field UHF tags could promise smaller sizes. In these applications the goal is to create very small activation regions, for instance by using conventional far field UHF tags and a reader with low transmitted power such that each tag will respond only when placed in the close proximity of the reader, Conversely, the reader could radiate the same power, as in the far field applications, but the tag impedance is mismatched so that it responds only to strong fields in the vicinity of reader antenna. Both these two options have, however, the drawback to not permit any size reduction of the tag (first case) and to produce a non localized interrogation zone (second case) so that the reader may un-intentionally see some other long range tags present in the far field region.

More efficient tag design consists in introducing a coil element to create a strong near field magnetic coupling with the reader, as in the case of LF systems. Due to the higher working frequency than in the LF band, the coil size required to the UHF tags could be considerably smaller than in the case of LF tags. Moreover such a coil could be also integrated with a dipole-like antenna, as the T-match or the inductively

coupled loop layouts described in Section 2. When properly optimized, such layouts could be used in both near and far field regions.

The design of near field UHF tags deserves in any case particular complexity since the electromagnetic coupling between the reader and the tag, due to the mutual small distance, may not be neglected, the antenna performance parameters (gain and impedance) can not be specified independently, and therefore the whole system needs to be studied by means of numerical electromagnetic solvers such as the Method of Moments, or the Finite Difference Time Domain [46].

5. Tag measurement and testing

The measurement of tag performance is a not yet assessed issue, as instead in case of more conventional 50-Ω-matched antennas. The tag is in fact designed to work as back-scattering antenna and it is connected to the microchip which is a non-linear load. Three different measurement strategies are typically adopted: *i)* measurement of the chipless tag's input impedance and gain, *ii)* measurement of the tag radar cross-section for different loading impedances, and *iii)* measurement of the read distance when a reader-tag link is established. In all the cases, since the tag is designed to be attached onto a class of targets, a reference object should be included in the measurement to have reliable data.

5.3 Measurement of input impedance and gain

This is the most general measurement of the specific tag performances. The critical issue is the connection of the Vector Network Analyzer (VNA) probe to the tag terminals, in absence of the microchip. Since the tag is not designed as a transmitting antenna, a balanced connection of the VNA coaxial cable to the tag port often requires a balun or a choke. In this case, particular care has to be devoted to avoid impedance and pattern distortion. Accurate measurement's schemes can be achieved in case the tag is a grounded antenna, as in the case of some (P)IFA-like structure previously described, or when the tag possesses an electric symmetry plane. Under this last condition, only half the antenna needs to be fabricated and the VNA probe can be placed in the ground plane's side which is opposite to the antenna half-space. For instance Figure 17 shows the measurement setup [21] of the NSSP antenna reviewed in Figure 6.

The antenna gain can be measured by standard techniques and all the tag's performance indicators (realized gain, bandwidth, reading distance) can be then calculated in post processing and are scenario- and reader-independent.

5.2 Measurement of the tag radar cross-section

A relevant part of reader-tag communication consists of tag's backscattering of the continuous wave coming from the reader. During this task, the microchip acts as a programmable switching device which connects or disconnects the antenna to a Z_{mod} load (typically an open circuit or high impedance for low state, and a short circuit or the antenna conjugate impedance, for the high state). During the data transfer, the RFID system can be considered as a monostatic radar and therefore it can be characterized by the radar cross-section (RCS) σ_T. As detailed discussed and experimentally verified in [47], the RCS of many classes of tag antennas can be easily related to the antenna gain and input impedance as

$$\sigma_T = \frac{\lambda^2 G^2 R_A}{\pi \left| Z_A + Z_{\mathrm{mod}} \right|^2} \tag{6}$$

The RCS of the chipless tag can be then measured as the S_{11} variation at the port of an illuminating antenna in both an anechoic chamber or a real scenario. The measurements is generally repeated for different impedances Z_{mod}. Although this is an indirect measures, which does not give any direct information about input impedance and the activation range, it is nevertheless a reader-independent characterization.

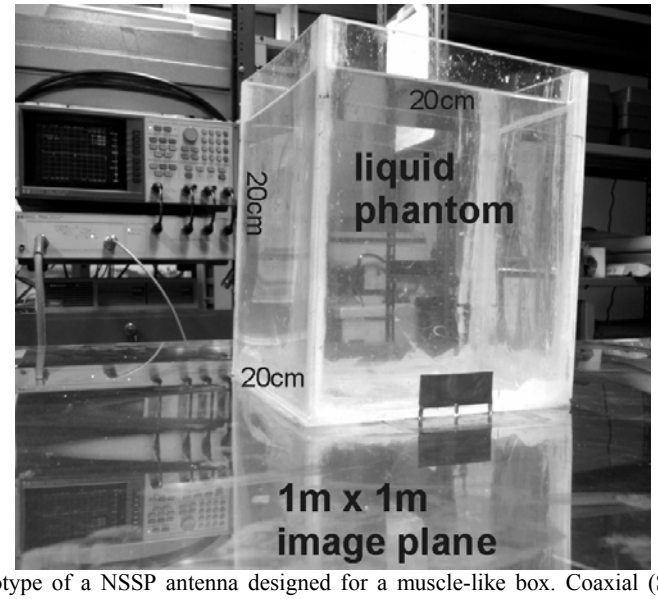

Figure 17: Copper prototype of a NSSP antenna designed for a muscle-like box. Coaxial (SMA) connector is in the reverse side of the image plane.

5.3 Measurement of the reading distance

This is an application- and scenario-specific measurement since, beside the choice of the target, it is strictly related to the reader features and to the transmitting power and requires to physically connect a particular microchip at the tag antenna's port [48]. Measurements can be also performed in a controlled environment such as an anechoic camber or a TEM cell, as detailed described in [10] and typical diagrams of reading range with respect to distance and reader power are generally produced.

This measurement is the simplest to perform. In case of real scenarios, it does not requires any particular and expensive equipment, beside a reader, and provides a true system performance evaluation. However the features of the tag itself are hidden within the overall results and therefore this procedure is of less general meaning than the previous measurement schemes.

4. Concluding remarks

Several kinds of basic design layouts have been discussed. The MLA configurations exhibit the largest number of degrees of freedom which can be globally optimized to suite the tag to a large variety of microchips ad sizes. Also the tagged object could be accounted for in the antenna design procedure by employing layered media models. The (P)IFA structures are instead particular attractive for metallic objects, while the Nested-Slot Suspended-Patch antenna could be useful (besides the (P)IFA) to host sensors and electronics.

The available know-how, scattered all over the open technical literature, seems to be enough mature and rich to approach the design of conventional UHF passive RFID tags. Due to the general small-size requirements, the resulting antenna bandwidth is however narrow, no matter which configuration is chosen, and therefore the antenna performances are strongly dependent on the nearby environment. The open challenge is therefore the design of antennas whose input and radiation properties remain nearly unchanged when the tag is attached onto different substrates such as paper, wood, metal, or living tissues. The problem is particular hard in the presence of metals and the (P)IFA-like structures give only a partial solution.

Further research effort could be devoted to the design methodology of RFID tag antennas for Sensor Networks, where the tag should by tightly integrated with sensor and electronics.

5. Acknowledgments

The author wishes to thank Claudio Calabrese for his enthusiastic and valuable support in documentation and computer simulations.

6. References

[1] H. Stockman "Communication by Means of Reflected Power" *Proceedings of the IRE*, **36**, 10**.** October 1948, pp. 1196-1204.

[2] J. Landt, "The History of RFID," *IEEE Potentials*,. **24**, 4, October-November. 2005, pp. 8-11.

[3] A. R. Koelle, S. W. Depp, and R. W. Freyman, "Short-Range Radio-Telemetry for Electronic Identification, Using Modulated RE Backscatter," *Proceedings of the IEEE*, **63**, 8, August 1975, pp.1260-1261.

[4] A. R. Koelle, "Short Range UHF Telemetry System Using Passive Transponders for Vehicle ID and Status Information", *IEEE Workshop on Automotive Applications of Electronics*, Dearborn MI, October 1988, pp.34-38.

[5] K. Finkenzeller, *RFID Handbook*, Wiley & Son, New York, 2000

[6] R. Want, "An Introduction to RFID Technology," *IEEE Pervasive Computing*, **I.5**, 1, January-March 2000, pp. 25-33.

[7] R. Bansal, "Coming soon to a Wal-Mart near you," *IEEE Antennas Propagayion. Magazine* **45**, 6, December 2003, pp. 105–106.

[8] S. Nambi, S. Nyalamadugu, S. M. Wentworth and B. A. Chin, "Radio frequency identification sensors", *Proc. 7th World Multiconf. Systemics, Cybernetics & Informatics* (SCI 2003), Orlando, FL, June 2003, pp.386-390.

[9] R. S. Sangwan, R. G. Qiu and D. Jessen "Using RFID tags for tracking patients, charts and medical equipment within an integrated health delivery network", *IEEE Int. Conf. Networking Sensing and Control,* 2005, pp.1070-1074.

[10] K. V. S. Rao, P. V Nikitin and S. F. Lam, "Antenna design for UHF RFID tags: A review and a practical application", *IEEE Transaction on Antennas and Propagation,* **53**, 12, December 2005, pp. 3870- 3876.

[11] J. Curty, N. Joehl, C. Dehollain and M. J. Delercq, "Remotely powered addressable UHF RFID integrated system", *IEEE Journal of Solid-State Circuits*, **40**,.11, November 2005, pp. 2193-2202.

[12] S. Basat, S. Bhattacharya, A. Rida, S. Johnston, L. Yang, M.M. Tentzeris and J. Laskar ,"Fabrication and Assembly of a Novel High-Efficiency UHF RFID Tag on Flexible LCP Substrate", *Electronic components and Technology Conference*, May-June 2006, pp.1352-1355.

[13] H.W. Son, J. Yeo, G.Y. Choi, and C.S. Pyo, "A Low-Cost, Wideband Antenna for Passive RFID Tags Mountable on Metallic Surfaces", *Proc. of the IEEE Antennas and Propagation Society Symposium*, Albuqueque, NM, June 2006, pp.1019-1022.

[14] S. Uda, Y. Mushiake, *Yagi-Uda Antenna*, Sasaki Printing and Publishing Co. Japan, 1954, pp.119-131.

[15] C. A. Balanis, *Antenna Theory. Analysis and Design*, Second Edition, John Wiley & Sons Inc., 1997.

[16] L. Ukkonen, M. Schaffrath, J.a Kataja, L. Sydanheimo and M. Kivikoski, Evolutionary RFID tag antenna design for paper industry applications, *International Journal of Radio Frequency Identification Technology and Applications*, **1**, 1, January 2006, pp.107-122.

[17] H. W. Son and C.S. Tyo, "Design of RFID tag antennas using an inductively coupled feed", *Electronics Letters*, **41**, 18, , September 2005, pp. 994-996.

[18] Y. Lee, "Antenna Circuit Design for RFID Applications", *Application Note AP710 of Microchip Technology Inc.* 2003, available online up to 1 Nov.2006 at *ww1.microchip.com/downloads/en/AppNotes/00710c.pdf*.

[19] "*FEKO User's Manual, Suite 5.1*", EM Software & Systems-S.A. (Pty) Ltd., Stellenbosch, South Africa, December. 2005, available online at http://www.feko.info.

[20] G. Marrocco, "Body-matched antennas for wireless biometry", *European Conference on Antennas and Propagat*, Nice (France), November 2006, p.795.

[21] G. Marrocco, "Rfid antennas for the UHF remote monitoring of Human subjects", *IEEE Transaction on. Antennas and Propagation*, **55**, 6, June 2007, pp. 1862-1870.

[22] G.Marrocco and C. Calabrese, "Automatic design of miniaturized slot-line RFID antennas", *2th European Conference on Antennas and Propagation (EUCAP)*, Edimburg (Scotland), November 2007.

[23] D.S. Weile and E. Michielsen, "Genetic algorithm optimization applied to electromagnetics: a review", *IEEE Transaction on Antennas and Propagation*, **45**, 3, March 1997, pp.343-353.

[24] G. Marrocco, "Gain-optimized self-resonant meander line antennas for RFID applications", *IEEE Antennas and Wireless Propagation Letters*, **2**, 2003, pp.302-305.

[25] N. Michishita and Y. Yamada, "A Novel Impedance Matching Structure for a Dielectric Loaded 0.05 Wavelength Small Meander Line Antenna", *IEEE Antennas and Propagation Society, International Symposium*, Albuquerque, NM, July 2006, pp. 1347-1350.

[26] W. Choi, H. W. Son, C. Shin, J.-H. Bae and G. Choi, "RFID tag antenna with a meandered dipole and inductively coupled feed", *IEEE Antennas and Propagation Society, International Symposium*, Albuquerque, NM, July 2006, pp. 619-622.

[27] A. Toccafondi and P.Braconi, "Compact load-bars meander line antenna for UHF RFID transponder", *European Conference on Antennas and Propagation,* Nice (France), November 2006, p. 804,

[28] S. A. Delichatsios, D. W. Engels, L. Ukkonen and L. Sydänheimo, "Albano multidimensional UHF passive RFID tag antenna designs", *Int. J. Radio Frequency Identification Technology and Applications*, **1**, 1, January 2006, pp. 24-40.

[29] C. Cho, H. Choo and I. Park, "Design of Novel RFID Tag Antennas for Metallic Objects", *IEEE Antennas and Propagation Society International Symposium*, Albuquerque, NM, July 2006, pp. 3245-3248.

[30] M. Keskilammi and M. Kivikoski, "Using Text as a Meander Line for RFID Transponder Antennas", *IEEE Antennas and Wireless Propagation Letters*, **3**, 2004, pp. 372-374.

[31] Y. Tikhov, Y. Kim and Y.-H. Min, "Compact Low Cost Antenna for Passive RFID Transponder", *IEEE Antennas and Propagation Society, International Symposium*, Albuqueque (NM), July 2006, pp. 1015-1018.

[32] C. Soras, M. Karaboikis, G. Tsachtsiris and V Makios, **"**Analysis and design of an inverted-F antenna printed on a PCMCIA card for the 2.4 GHz ISM band", *IEEE Antennas and Propagation Magazine*, **44**, 1, February 2002, pp.37-44.

[33] H. Hirvonenen, P. Pursula, K. Jaakkola and K. Laukkanen, "Planar inverted-F antenna for radio frequency identification", *Electronics Letters,* **40,** 14, July 2004, pp.848-850.

[34] B. Yu, S.-J. Kim, B. Jung, F. J. Harackiewicz, M.-J. Park and B. Lee, "Balanced RFID Tag Antenna Mountable on Metallic Plates", *2006 IEEE Antennas and Propagation Society, International Symposium*, Albuquerque, NM, July 2006 pp. 3237-3240.

[35] C. H. Cheng and R. D. Murch, "Asymmetric RFID Tag Antenna", *2006 IEEE Antennas and Propagation Society, International Symposium*, Albuquerque, NM, July 2006, pp.1363-1366.

[36] I.Y. Chen, C.U. Huang, H.H.J. Chen, C.F. Jou and S.R.S. Huang, "Folded dual-band (2.4/5.2 GHz) antenna fabricated on silicon suspended parylene membrane", *Asia Pacific Microwave Conference Proceedings* December 2005, **4**, pp.4-8, 2005.

[37] X. H. Wu and Z. N. Chen , "Comparison of planar dipoles in UWB applications", *IEEE Transaction on Antennas and Propagation*, **53**, 6, June 2005, pp. 1973- 1983.

[38] C. Diugwu, J.C. Batchelor, "Analysis of the surface distribution in a dual band planar antenna for passive RFID tag", *IEEE Antennas and Propagation Society, International Symposium*, Washington, NY, July 2005, pp.459-462.

[39] S. Tedjini, T. Voung, and V. Beroulle, "Antennas for RFID tags", *Joint sOc-EUSAI conference*, Grenoble, France, 2005, pp.19-22.

[40] S. Jeon, Y. Yu, S. Kahng, J. Park, N. Kim and J. Choi, "Dual-band Dipole Antenna for ISO 18000-6/ISO 18000-4 Passive RFID Tag Applications", *IEEE Antennas and Propagation Society, International Symposium*, Albuqueque (NM), July 2006, pp.4285-4288.

[41] L. Mattioni and G. Marrocco, "BLADE: A Broadband Loaded Antennas DEsigner", *IEEE Antennas Propagat.Magazine*, **48**, 5, October 2006, pp.120 - 129.

[42] M. Hirvonen, K. Jaakkola, P. Pursula and J. Saily, "Dual-band platform tolerant antennas for Radio-Frequency Identification", *IEEE Transaction on Antennas and Propagation*, **54**, N.9, September 2006, pp.2632-2636.

[43] S. Nambi and S. M. Wenthworth, "5.8 GHz dual-polarized aperture-coupled Microstrip antenna", *IEEE Antennas and Propagation Society, International Symposium*, Washington, NY, July 2005, pp.235-238.

[44] M. Stupf, R. Mittra, J. Yeo and J.R. Mosig, "Some novel design for RFID antennas and their performance enhancement with metamaterials", *IEEE Antennas and Propagation Society, International Symposium*, Albuqueque, NM, July 2006, pp.1023-1026.

[45] P. V. Nikitin, K.V. Rao and S. Lazar, "An overview of Near Field UHF RFID", *IEEE Int. Conf. on RFID,* March 2007, pp. 167-173.

[46] A. Taflove, *Computational electromagnetics: The Finite difference method*, Artech House, Norwood, MA, 1995

[47] P. Nikitin and K.V.S. Rao, "Theory and measurement of backscattering from RFID tags", *IEEE Antennas and Propagation. Magazine.*, **48**, 6, Dec. 2006, pp.212-218.

[48] L. Ukkonen, L. Sydänheimo and M. Kivikoski "Effects of Metallic Plate Size on the Performance of Microstrip Patch-Type Tag Antennas for Passive RFID", *IEEE Antennas Wireless Propagation. Letters*., **4**, 2005, pp.410-413.

Biography

Photo_marrocco.jpg

Gaetano Marrocco (M'98) received the Laurea degree in electronic engineering and the Ph.D. degree in applied electromagnetics from the University of L'Aquila, Italy, in 1994 and 1998, respectively. Since 1997, he has been a Researcher at the University of Rome "Tor Vergata," Rome, Italy, where he currently teaches Antenna Design and Bioelectromagnetics. In summer 1994, he was at the University of Illinois at Urbana-Champain as a Postgraduate Student. In autumn 1999, he was a Visiting Researcher at the Imperial College in London, U.K.. His research is mainly directed to the modelling and design of broad band and ultra wideband antennas and arrays as well as of miniaturized antennas for RFID applications. He has been involved in several space, avionic, naval and vehicular programs of the European Space Agency, NATO, Italian Space Agency, and the Italian Navy. He holds two patents on broadband naval antennas and one patent on sensor RFID systems. He currently serves as Associate Editor of the IEEE Antennas and Wireless Propagation Letters.